A Monte Carlo Study of the Evolution of the Scale Height of Normal Pulsars in the Galaxy *

Ying-Chun Wei[1], Xin-Ji Wu[2,1], Qiu-He Peng[3], Na Wang[1] and Jin Zhang[1]

[1] National Astronomical Observatories/Urumqi Observatory, Chinese Academy of Sciences, Urumqi 830011

[2] Department of Astronomy, Peking University, Beijing 100871; *wuxj@bac.pku.edu.cn*

[3] Department of Astronomy, Nanjing University, Nanjing 210093

Abstract Based on the undisturbed, finite thickness disk gravitational potential, we carried out 3-D Monte Carlo simulations of normal pulsars. We find that their scale height evolves in a similar way for different velocity dispersions (σ_v): it first increases linearly with time, reaches a peak, then gradually decreases, and finally approaches a stable asymptotic value. The initial velocity dispersion has a very large influence on the scale height. The time evolution of the scale height is studied. When the magnetic decay age is used as the time variable, the observed scale height has a similar trend as the simulated results in the linear stage, from which we derive velocity dispersions in the range $70 \sim 178 \, \mathrm{km \, s^{-1}}$, which are near the statistical result of $90 \sim 270 \, \mathrm{km \, s^{-1}}$ for 92 pulsars with known transverse velocities. If the characteristic age is used as the time variable, then the observed and theoretical curves roughly agree for $t > 10^8$ yr only if $\sigma_v < 25 \, \mathrm{km \, s^{-1}}$.

Key words: pulsar: general – stars: evolution – Galaxy: structure – Galaxy: disk

1 INTRODUCTION

The distributions of celestial objects of different kinds in the Galaxy have always been studied with much effort, such as pulsars, SNRs (Xu et al. 2005; Leahy & Wu 1989; Wu & Leahy 1988), SiO and OH (Jiang & Jia 2001). However, except these direct observation data analysis, numerical calculation techniques are also widely used. So far in the study of pulsars' distribution in the Galaxy, many authors have utilized the method of Monte Carlo simulation. Zhao & Huang (1992) adopted the gravitational potential of Rohlfs & Kreitschmann (1981), but let the galactocentric radius r (the projective distance of pulsars on the Galactic plane from the galactic center) to be fixed, so their simulation was a 1-D simulation. Sun & Han (2004) performed detailed 3-D Monte Carlo simulation adopting Paczynski's gravitational potential. The pulsar's

birthrate was reckoned in Zhao & Huang (1992). Sun & Han (2004) considered the pulsars were not born one by one, but rather, in groups.

Because pulsars originate from OB-stars in the galactic disk, their motions are strongly affected by the gravitational potential of the galactic disk. The effect of a finite thickness of the disk should be considered, so here we adopt the gravitational potential for an undisturbed finite thickness disk obtained by Peng et al. (1978) in our 3-D Monte Carlo simulations of the pulsar distribution. We used the Paczynski gravitational potential to calculate the pulsars' initial circular velocities.

In Section 2 we describe the details of our simulation, including the gravitational potential, the initial position distribution of pulsars, and velocity distribution and birthrate. The results are reported in Section 3. In Section 4 the results are compared with the observed evolution of scale height of normal pulsars. The statistics of the observed velocity distribution of normal pulsars is given in Section 5.

2 INITIAL CONDITIONS AND METHOD OF SIMULATION

The initial positions and velocities of pulsars are chosen by Monte Carlo. For these initial conditions, the differential equations of pulsars' motion in the galactic gravitational field were followed to obtain their locations at other times.

2.1 Gravitational Potential

The gravitational potential for the undisturbed finite thickness disk derived by Peng et al. (1978) can be cast in the form:

$$\phi(r,z) = -\pi G\alpha \int_0^\infty J_0(\beta r)S(\beta)\frac{2}{\beta^2-\alpha^2}(\beta e^{-\alpha|z|} - \alpha e^{-\beta|z|})d\beta\,,$$

$$S(\beta) = \int_0^\infty rJ_0(\beta r)\sigma(r)dr\,,$$

(1)

where G is the gravitational constant; $\alpha = 1/h_z$, h_z is the scale height of the galactic disk; $\sigma(r) = \sigma_0 e^{-\frac{r}{h_d}}$ is the surface density, h_d is the scale length of the galactic disk. In the simulation, we adopt h_d=4.7 kpc, $\sigma(R_0) = 52.1\,M_\odot$ pc^{-2} (Hartman et al. 1997; Sun & Han 2004), R_0=8.0 kpc is the distance between the Sun and the Galactic center following Sun & Han (2004), and h_z=0.325 kpc is the scale height of the Galactic disk.

2.2 Coordinate System and Pulsar Birthrate

As in Sun & Han (2004), we adopt a rectangular coordinate system (origin galactic centre) with the x, y-axes in the galactic plane and the z-axis perpendicular to it. Obviously the simulation results are independent of the coordinate system adopted. The pulsars were born one by one according to the birthrate. The birthrate of normal pulsar is one per 60 to 330 yr, as suggested by Manchester (2001), so the median value of birthrate is one per 195 yr. There are four spiral arms in the Galaxy, and the birthrate is one per 780 yr in each spiral arm.

2.3 Initial Birthplace

In our simulation, the vertical distances (z) of the pulsars' birthplaces from the Galactic plane are defined by the exponential distribution $\lambda e^{-\lambda|z|}$, where λ=1/0.07 kpc^{-1} on supposing that the pulsars are born from a population with a scale height of 0.07 kpc (Gunn & Ostriker 1970). The projected pulsars' birthplaces on to the galactic plane lie in a spiral arm and the projected radial distances (r) from the Galactic center are in the range 4.0–25.0 kpc. This is because

there are four Galactic spiral arms lying symmetrically in the Galactic plane outside the limit $r_0 = 4.0$ kpc which marks the forbidden radius of density wave in the Galaxy (Tong et al. 1982). Moreover, it is expected that the pulsars' birth probability is proportional to the surface density of the spiral arm where it is born. The logarithmic spiral arm is represented by

$$\sigma_1(r, \theta, t) = \frac{A}{r} e^{i\Lambda \ln(r)} e^{i(\omega t - m\theta)},$$
(2)

where $\Lambda = m \cot(\mu)$, $m = 4$ is the number of spiral arms in the Galaxy, μ is the pitch angle of the spiral arms, $\Lambda = 14.0 \pm 0.5$, $\omega = 0.00527'' \text{ yr}^{-1}$ is the angular velocity of the Galaxy, and A is a constant for the distribution.

2.4 Initial Velocity Distribution

The initial velocity of each pulsar is the vector sum of the circular rotation velocity at the birth position and a random velocity from the supernova explosion. The circular rotation velocity is given by

$$v_{\text{circ}} = \left(r \frac{d\Phi}{dr} \right)^2,$$
(3)

$$\Phi = \Phi_{\text{sph}} + \Phi_{\text{disk}} + \Phi_{\text{halo}},$$
(4)

where Φ_{sph}, Φ_{disk} and Φ_{halo} respectively denote the spheroidal, disk and halo components of galactic gravitational potential given by Paczynski (1990) as

$$\Phi_i(r, z) = \frac{GM_i}{\sqrt{r^2 + [a_i + (z^2 + b_i^2)^{1/2}]^2}}, \qquad r^2 = x^2 + y^2,$$
(5)

where $a_{\text{sph}} = 0.0$ kpc, $b_{\text{sph}} = 0.277$ kpc and $M_{\text{sph}} = 1.12 \times 10^{10} M_\odot$ for the spheroidal component, $a_{\text{disk}} = 3.7$ kpc, $b_{\text{disk}} = 0.200$ kpc and $M_{\text{disk}} = 8.01 \times 10^{10} M_\odot$ for the disk component. The halo component is given by

$$\Phi_{\text{halo}} = -\frac{GM_{\text{halo}}}{r_c} \left[\frac{1}{2} \ln \left(1 + \frac{r^2 + z^2}{r_c^2} \right)^2 + \frac{r_c}{\sqrt{r^2 + z^2}} \arctan \left(\frac{\sqrt{r^2 + z^2}}{r_c} \right) \right], \qquad r^2 = x^2 + y^2,$$
(6)

where $r_c = 6.0$ kpc, $M_{\text{halo}} = 5.00 \times 10^{10} M_\odot$. As in Sun & Han (2004), the pulsar random velocities are chosen from a 3-D isotropic Maxwellian distribution with different velocity dispersion.

2.5 Equation of Pulsar Motion

We solve the differential equations of pulsars' motion in the Galactic gravitational field following the method given in Sun & Han (2004). The differential equations may be cast in the compact form

$$\ddot{\boldsymbol{r}}(t) = -\boldsymbol{\nabla}\phi(\sqrt{x^2 + y^2}, z).$$
(7)

The pulsar orbits were numerically integrated with a fourth-order Runge-Kutta method as in Paczynski (1990).

3 SIMULATED RESULT OF SCALE HEIGHT EVOLUTION OF $|z|$ DISTRIBUTION OF PULSARS

The z-distribution of the pulsars is approximately an exponential curve, the value at $1/e$ of z distribution curve is the scale height of z distribution. However, the mean value of z also used to represent the scale height (Zhao & Huang 1992). In this paper we adopt the cumulative scale

height (h_z) to study the evolution. The scale heights in a given age segment show oscillations with time, while the evolution of the cumulative scale height (h_z) is smoother and has a better linear relationship with time for times that are too long ($< 2 \times 10^7$ yr).

We have carried out 3-D Monte Carlo simulations of 4×10^5 pulsars in the range of $r = 4.0 - 25.0$ kpc for different velocity dispersions σ_v. The mode of one exponential decay is used to fit the height z distribution describing the cumulative scale height (h_z) for certain age segment in the range $r = 5.0 - 11.0$ kpc. The evolution of h_z shown in Figure 1 has common trend and similar shape for different σ_v: it first increases linearly with time, reaches a peak, then keeps falling toward a constant value. A similar evolution shape was derived by Zhao & Huang (1992) and Sun & Han (2004), but the durations of the linear stage are different: Zhao & Huang (1992) had 10 Myr, Sun & Han (2004) had 40 Myr and we have 30 Myr.

For large σ_v (> 110 km s^{-1}) the peaks of cumulative scale height (h_z) exceed 1 kpc, and the final steady values remain above 0.7 kpc, which is obviously inconsistent with the observations. For small $\sigma_v (< 50$ km s^{-1}) the peaks are less than 0.5 kpc, and the final values are less than 0.4 kpc; but such small $\sigma_v (< 50$ km s^{-1}) values are inconsistent with the observations.

The correlations between h_z and σ_v at $t = 8 \times 10^5$, 4×10^6, 7×10^6 and 10^7 yr are shown in Figure 2. The correlation is approximately linear. If the lifetime of pulsars is not too long, e.g., about 10^7 yr, and if σ_v is about 100 km s^{-1}, then the corresponding h_z is 0.4 kpc . In order to make a comparison with the observations, we need to study the pulsar lifetime and true age.

4 COMPARISON WITH OBSERVATION

4.1 Statistical Samples

Up to now more than 1500 pulsars have been detected in the Galaxy[1]. Because of the pulsar intrinsic luminosity, the beam factor and interstellar absorption, scattering and dispersion, there are difficulties in the discovery of pulsars, especially when they are very far from us. Selection effect of the survey must be considered (Wu & Leahy 1989; Arzoumanian et al. 2002).

We restricted our study to the range $5 < r < 11.0$ kpc, because in the vicinity of the Galactic center the observation are too sparse. There are 824 pulsars in the above range with known characteristic ages τ. When the millisecond pulsars, the binary pulsars and the millisecond-pulsar-like pulsars (Wu et al. 1991; Kuzmin & Wu 1992) are excluded, the sample includes 750 pulsars. This sample includes all pulsars in the vicinity of the Sun, some more distant ones. We selected a second statistical sample of 291 pulsars with distances from the Sun $d < 3.0$ kpc; this sample has a sufficient size.

4.2 Correlation between Pulsar Scale Height and Characteristic Age

We use the mode of one exponential decay to fit the distribution of their heights, and plot the cumulative scale height (h_z) versus $\log_{10}(\tau)$ (τ is characteristic age) in Figure 3. Two theoretical curves for $\sigma_v = 25$ km s^{-1} and 30 km s^{-1} are also plotted in Figure 3.

The agreement between the theoretical and the observational curves in Figure 3 is not good. There exists a roughly similar trend for $t > 10^8$ yr for $\sigma_v < 25$ km s^{-1}, but such a small σ_v obviously contradicts the observation (see Section 5).

4.3 Relationship between Pulsar Scale Height and Magnetic Decay Age

Many authors have earlier suggested that the pulsar characteristic age is not its true age, while magnetic decay age or dynamic age can represent the true age. The correlation between the

---

[1] http://www.atnf.csiro.au/research/pulsar/catalogue/
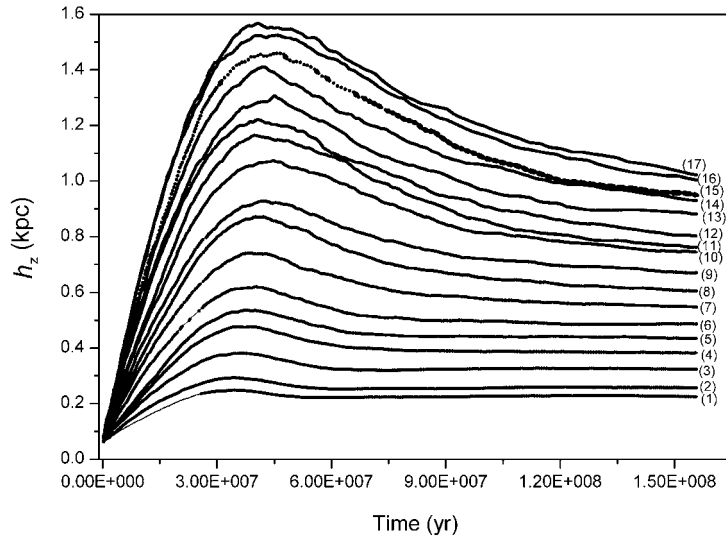
Fig. 1 Cumulative scale height evolution of pulsars in the galactocentric radius r range 5.0–11.0 kpc. The number of (1) to (17) refer to different dispersions σ_v in the initial isotropic Maxwellian velocity distribution: 25, 30 , 40, 50, 60, 70, 83, 95, 110, 125, 140, 155, 168, 178, 185, 195 and 205 km s^{-1}.
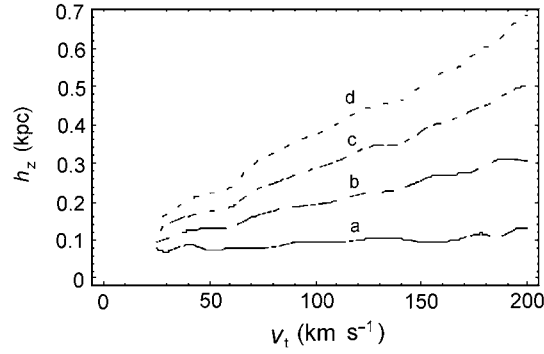
Fig. 2 Correlations between the cumulative scale height (h_z) and initial isotropic Maxwellian velocity dispersion σ_v at times $t = 8 \times 10^5$ (a), 4×10^6 (b), 7×10^6 (c) and 10^7 yr (d).

pulsar's characteristic age τ and the magnetic decay age t can be

$$t = \frac{\tau_D}{2} \ln \left(\frac{2\tau}{\tau_D} + 1 \right). \tag{8}$$

Some authors have used the statistics of pulsars to derive the magnetic decay constant τ_D, e.g., $\tau_D = 1.6 \times 10^6$ yr (Qu et al. 1976), 5×10^6 yr (Lyne et al. 1998), 9×10^6 (Lyne et al. 1985) and 1.5×10^7 yr (Xu & Wu 1991).

Many studies have shown that the pulsar's magnetic inclination gets smaller with time, leading to the vertical magnetic moment getting smaller with time (Wu et al. 1982; Qiao et al.
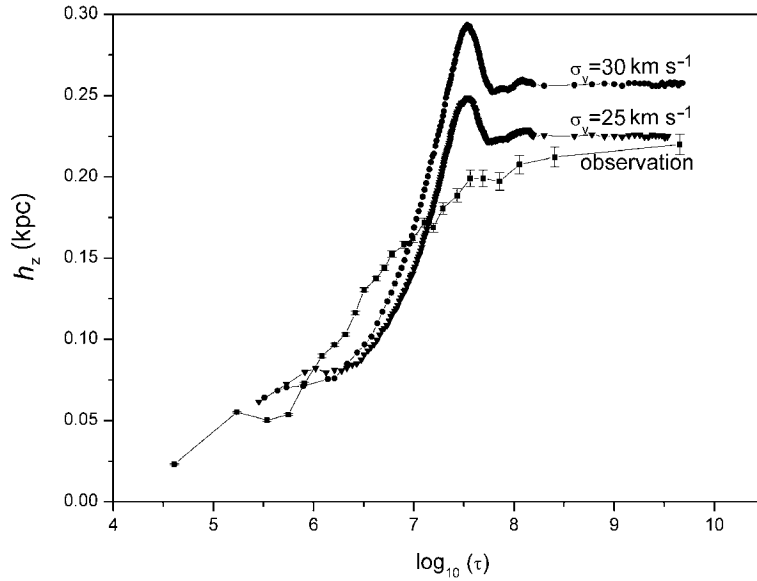
Fig. 3 Evolution of the cumulative scale height of 750 pulsars in $5.0 < r < 11.0\,\mathrm{kpc}$ with $\log_{10}(\tau)$.

1986; Kuzmin & Wu 1992; Zhang et al. 1992, 1998). This is probably the important factor for the magnetic decay of pulsars. The comparatively smaller τ_D means the true age of pulsar and the lifetime being smaller. The initial velocity dispersion can take a larger value, which is required by the simulated $h_z(\sigma_v, t)$. For several values of τ_D given by different authors, the curves of the cumulative scale height for our first pulsar sample ($5 < r < 11.0\,\mathrm{kpc}$) with magnetic decay age are plotted in Figure 4. Six theoretical curves with $\sigma_v = 25, 30, 70, 95, 178$ and $185\,\mathrm{km\ s^{-1}}$ derived from Figure 1 are also plotted for comparison. The second pulsar sample ($d < 3\,\mathrm{kpc}$) give very similar curves as the first sample.

The observed curves are consistent with the simulated curves with $\sigma_v = 178, 95$ and $70\,\mathrm{km\ s^{-1}}$ only in the initial linear stage for the cases of $\tau_D = 1.6 \times 10^6, 5 \times 10^6, 9 \times 10^6$ and $1.5 \times 10^7\,\mathrm{yr}$. This means that the observations are consistent with the theoretical results only for comparatively young pulsars. Because the magnetic decay constant τ_D is less than $1.5 \times 10^7\,\mathrm{yr}$, the pulsar's lifetime can not be too long.

5 STATISTICS OF TRANSVERSE VELOCITIES OF 92 PULSARS

The first sample of 750 pulsars includes 92 with known transverse velocities. The second sample of 291 pulsars ($d < 3\,\mathrm{kpc}$) includes 72. The transverse velocity is the projection of the absolute 3-D velocity onto the plane normal to the sight line. We can acquire its distribution from the one-component 3-D Maxwellian velocity distribution as follows: the latter is

$$f(v_x, v_y, v_z)dv_x dv_y dv_z = (\tfrac{A}{\pi})^{3/2} e^{-A(v_x^2 + v_y^2 + v_z^2)} dv_x dv_y dv_z, \qquad A = \tfrac{1}{2\sigma_v^2}. \qquad (9)$$

We integrate out one dimension, and derive the distribution of the 2-D absolute velocity value probability density

$$g(v_t)dv_t = \left[\int_{-\infty}^{\infty} 2\pi v_t f(v_x, v_y, v_z)dv_z \right] dv_t = 2Av_t e^{-Av_t^2} dv_t, v_t = \sqrt{v_x^2 + v_y^2}. \qquad (10)$$
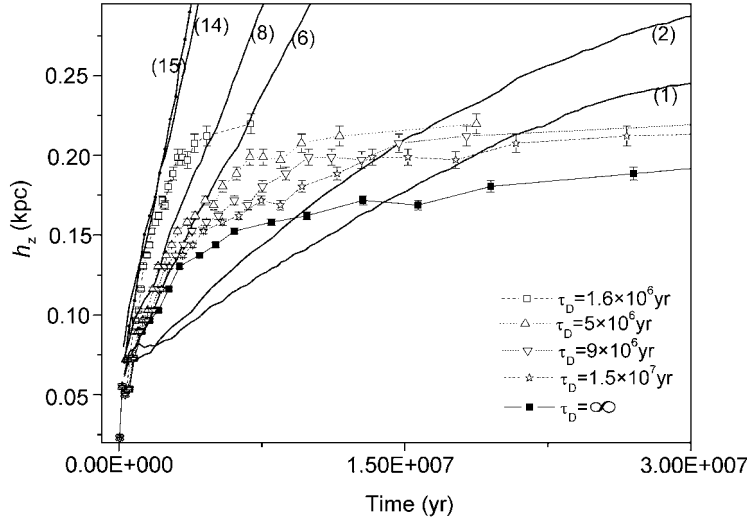
Fig. 4 Evolution of cumulative scale height of observed 750 normal pulsars in $5.0 < r < 11.0$ kpc, with five values of τ_D and six simulated curves derived from Fig. 1.

From Eq. (9), we obtain

$$
\sigma_v = \sqrt{\tfrac{1}{2A}} ,
$$
$$
\delta\sigma_v = -(\tfrac{1}{2A})^{3/2}\delta A . \tag{11}
$$

The two-component Maxwellian distribution of birth velocity with 1-D velocity dispersions $\sigma_v \sim 175\,\mathrm{km\ s^{-1}}$ and $700\,\mathrm{km\ s^{-1}}$ was suggested by Cordes & Chernoff (1998) and with 1-D velocity dispersions $\sigma_v \sim 90\,\mathrm{km\ s^{-1}}$ and $500\,\mathrm{km\ s^{-1}}$ by Arzoumanian et al. (2002). We also use the two-component Maxwellian distribution to fit the probability density distribution of the normalized transverse velocity of observed 92 pulsars. Equations (12) and (13) are the two-component Maxwellian distribution and the mean velocity in 3-D respectively:

$$
g_{\mathrm{two}}(v_t) = \frac{dN}{dv_t N}\Big|_{v_t=\sqrt{v_x^2+v_y^2}=\mathrm{const}} = 2cA1v_t e^{-A1v_t^2} + 2(1-c)A2v_t e^{-A2v_t^2} , \tag{12}
$$

$$
\overline{v} = c \cdot \sqrt{8/\pi} \cdot \sigma_{v1} + (1-c) \cdot \sqrt{8/\pi} \cdot \sigma_{v2} = 330.3 \pm 15.15\,(\mathrm{km\ s^{-1}}) , \tag{13}
$$

where c is the percentage of the component A1. We use $g_{\mathrm{two}}(v_t)$ to fit the probability density distribution of the normalized transverse velocity of the observed 92 pulsars in steps of $dv_t = 85\,\mathrm{km\ s^{-1}}$ to deserve A1, δA1 and A2, δA2, then use Equation (13) to calculate σ_{v1}, $\delta\sigma_{v1}$ and σ_{v2}, $\delta\sigma_{v2}$. The results are that σ_{v1} is $90.6\pm4.71\,\mathrm{km\ s^{-1}}$, σ_{v2} is $270.2\pm12.09\,\mathrm{km\ s^{-1}}$, and c is 35.2%. The fitted results are shown in Figure 5.

At present, there are three methods of measuring the pulsar velocity: pulse arrival time (Zou et al. 2005), radio interferometer and interstellar scintillation (Wang et al. 2001). Each method has its merits and shortcomings, but none of them can give the 3-D velocity of pulsars. The methods are all insensitive to far pulsars having comparatively small velocities. The method of interstellar scintillation can obtain the relative velocities of the pulsar and the scintillation screen and the earth. Because the velocity of scintillation screen is lacking, and the earth revolution speed is about $30\,\mathrm{km\ s^{-1}}$, this method is not effective when the pulsar proper motion is small.
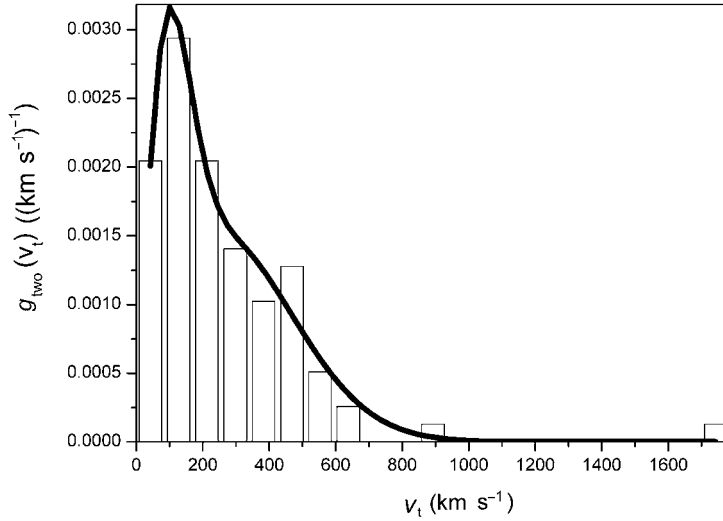
Fig. 5 Probability density distribution of normalized transverse velocity of observed 92 pulsars, and fitting result based on a two-component Maxwellian transverse velocity distribution function in steps of $dv_t = 85 \, \mathrm{km \, s^{-1}}$, with $\chi^2 = 1.5695 \times 10^8$ and $R^2 = 0.98172$.

Thus as to measurement of pulsar velocity, the ones with small velocities might be ignored, while the others with large velocities can be comparatively easily measured.

6 CONCLUSIONS

We summarize our work in this paper as follows:

(1) The evolution of the cumulative scale height is derived: the scale heights first increases linearly with time, after reaching a peak it gradually decreases and finally approaches a constant value. The initial velocity dispersion has a very large influence on the scale height. The trend above is basically similar to Sun & Han (2004), though our gravitational potential differs from theirs.

(2) For 92 pulsars having transverse velocities, we use a two-component Maxwellian distribution to fit their observed distribution and obtained velocity dispersions $\sigma_{v1} = 90.6 \pm 4.71 \, \mathrm{km \, s^{-1}}$ and $\sigma_{v2} = 270.2 \pm 12.09 \, \mathrm{km \, s^{-1}}$. These results are preliminary as the present data of pulsar transverse velocities are incomplete.

(3) In the study of the evolution of cumulative scale height we find that if the characteristic age is used as the time variable, then the theoretical and the observational curves show some similarity in the long run ($t > 10^8 \, \mathrm{yr}$) only for very small velocity dispersions ($\sigma_v < 25 \, \mathrm{km \, s^{-1}}$). Such small velocity dispersions obviously contradict the observations. If the magnetic decay age is used as the time variable, then the observed and simulated curves are fairly consistent during the initial linear stage, from which we derive an initial velocity dispersion of $70 \sim 178 \, \mathrm{km \, s^{-1}}$, near the observed values.

References

Arzoumanian Z., Chernoff D. F., Cordes J. M., 2002, ApJ, 568, 289

Cordes J. M., Chernoff D. F., 1998, ApJ, 505, 315

Hartman J. W., Bhattacharya D. et al., 1997, A&A, 322, 477

Jiang B. W., Jia S. M., 2001, ChJAA, 1, 144

Kuzmin A. D., Wu X. J., 1992, ApSS, 190, 209

Leahy D. A., Wu X. J., 1989, PASP, 101, 607

Lyne A. G., Manchester R. N., Taylor H. J., 1985, MNRAS, 213, 613

Lyne A. G., Francis G. S., Pulsar Astronomy, Cambridge University Press

Peng Q. H. et al., 1978, Acta Astron. Sin., 19, 182

Qiao G. J., Wu X. J., Zhang H. et al., 1985, Science Bulletin, 8, 1062

Qu Q. Y., Wang Z. R., Lu T. et al., 1976, Chinese Science Bulletin, 21, 176

Sun X. H., Han J. L., 2004, MNRAS, 350, 232

Tong Y., Wu S. G., Peng Q. H., 1982, Acta Astron. Sin., 23, 140

Wang N., Wu X. J., Manchester R. N. et al., 2001, ChJAA, 1, 421

Wu X. J., Wu F., Qiao G. J. et al., 1982, Chin. Astron. Astrophys., 6, 216

Wu X. J., Wu F., Qiao G. J. et al., 1982, Acta Astrophys. Sin., 2, 140

Wu X. J., Leahy D. A., 1989, Acta Astrophys. Sin., 9, 232

Wu X. J., Kuzmin A. D., He L. S., 1991, Proceeding of 3rd Chinese Acadmic of Sciences and Max-Plank
    Scoiety Workshop, p.129

Wu X. J., 2000, The Physics of Pulsar, The Lecture Note of Peking University

Wu X. J., Leahy D. A., 1988, In: Proceeding of IAU Colloq. 101, The Interaction of SNRs with
    Interstellar Medium, p.484

Xu J. W., Zhang X. Z., Han J. L., 2005, ChJAA, 5, 165

Xu W., Wu X. J., 1991, ApJ, 380, 550

Zhang C. M., Yang G. C., Chen F. P., Wu X. J., 1992, G.R.G., 24, 359

Zhang C. M., Cheng K. S., Wu X. J., 1998, A&A, 332, 569

Zhao Y. H., Huang K. L., 1992, Acta Astrophys. Sin., 12, 302

Zou W. Z., Hobbs G., Wang N. et al., 2005, MNRAS, 362, 1189